Letters

Accurate Steady-State Representation of a Doubly Fed Induction Machine

V. Seshadri Sravan Kumar and D. Thukaram, *Senior Member, IEEE*

***Abstract*—This letter presents an accurate steady-state phasor model for a doubly fed induction machine. The drawback of existing steady-state phasor model is discussed. In particular, the inconsistency of existing equivalent model with respect to reactive power flows when operated at supersynchronous speeds is highlighted. Relevant mathematical basis for the proposed model is presented and its validity is illustrated on a 2-MW doubly fed induction machine.**

***Index Terms*—DFIG, Doubly fed induction machine, steady-state equivalent circuit, wind generation.**

NOMENCLATURE

v_s, i_s, ψ_s	Stator voltage, current, and flux, respectively.
v_r, i_r, ψ_r	Rotor voltage, current, and flux, respectively, (referred onto stator side).
$L_{\sigma s}, L_{\sigma r}$	Leakage inductance of stator and rotor (referred onto stator side), respectively.
L_m	Mutual inductance.
R_s, R_r	Stator and rotor resistances, respectively.
$X_{\sigma s}, X_{\sigma r}$	Leakage reactance of stator and rotor (referred onto stator side), respectively.
β_r	Position of rotor reference axis with respect to stationary frame of reference.
β_s	Position of d-axis with respect to stationary frame of reference.
ω_s	Synchronous speed.

The prefixes d and q in the subscript indicate the components along d-axis and q-axis, respectively.

I. INTRODUCTION

DOUBLY fed induction machine (DFIM)-based wind energy conversion systems [1] and [2] constitute major share of wind generating units installed around the world. Flexibility in control and ability to operate at relatively wide range of speeds are a few advantages offered by DFIM-based wind turbine generators. At the heart of such generating unit is the DFIM controlled using back-to-back converters [3].

Mathematical models to analyze the performance of a DFIM during stand-alone operation or when interfaced with the grid are very well established in the literature [4]–[6]. Using these models, the steady- state and dynamic behavior of DFIM when interfaced with the grid has been extensively reported in [7]–[12]. In these models, steady-state equivalent circuit forms the basis for determining the initial condition to study the dynamic behavior of DFIM and to analyze its steady-state behavior. In this context, an accurate steady-state model consistent for all possible modes of operation is very essential. The existing steady-state model of DFIM does not accurately represent reactive power flows in the machine when analyzed for supersynchronous speeds. In this letter, an accurate steady-state model for DFIM operating at supersynchronous speeds is proposed.

Manuscript received February 4, 2015; revised March 31, 2015; accepted April 17, 2015. Date of publication April 21, 2015; date of current version May 22, 2015.

V. Seshadri Sravan Kumar and D. Thukaram are with the Department of Electrical Engineering, Indian Institute of Science, Bangalore 560012, India (e-mail: seshadri@ee.iisc.ernet.in; dtram@ee.iisc.ernet.in).

Color versions of one or more of the figures in this paper are available online at http://ieeexplore.ieee.org.

Digital Object Identifier 10.1109/TPEL.2015.2425140

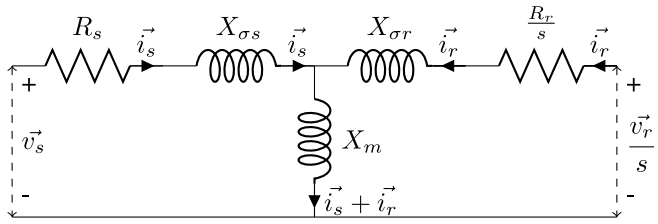

Fig. 1. Existing steady-state equivalent circuit of DFIM.

II. SHORTCOMINGS OF EXISTING EQUIVALENT CIRCUIT

The steady-state equivalent circuit of a DFIM proposed in the literature (using motor convention) is shown in Fig. 1. Given the active, reactive power P_s, Q_s, and the voltage $\vec{v_s}$ at the stator terminals, it is possible to compute [4] all the other variables of DFIM using the equivalent phasor model shown in Fig. 1. To illustrate the shortcomings of the existing equivalent circuit, a 2-MW DFIM (data given in Appendix[1]) is analyzed for its operation in all four quadrants. To make the inferences clear, the reactive power requirement at the stator terminals Q_s is presumed to be 0 Mvar (i.e., unity power factor (UPF) mode of operation). Further, the active power requirement at stator terminals P_s, the stator voltage $\vec{v_s}$, and the operating slip s are presumed to be ± 2 MW ($P_s = \pm 0.95$ p.u.), $\vec{v_s} = 1\angle 0$ p.u., and ± 0.25 ($s = \pm 0.25$), respectively.

Under this scenario, the active and reactive power requirement at the rotor side P_r, Q_r and the net mechanical torque T_m computed using the existing equivalent circuit for its operation in all the four quadrants is summarized in Table I. The corresponding phasor diagrams are illustrated in Fig. 2.

[1]In this letter, the analysis is carried out using per unit (p.u.) values. The base values of apparent power and voltage are given in Appendix.

TABLE I
ANALYSIS OF FOUR-QUADRANT OPERATION OF DFIM USING EXISTING EQUIVALENT CIRCUIT[1] ($Q_s = 0$, $s = \pm 0.25$) (ALL VALUES ARE IN P.U.)

Quad	ω_r	P_s	P_r	Q_r	P_m	T_m
A	$\omega_r < \omega_s$	0.95	−0.22	0.13	0.73	0.94
B	$\omega_r > \omega_s$	0.95	0.25	**−0.13**	1.20	0.94
C	$\omega_r > \omega_s$	−0.95	−0.22	**−0.13**	−1.18	−0.96
D	$\omega_r < \omega_s$	−0.95	0.25	0.13	−0.70	−0.96

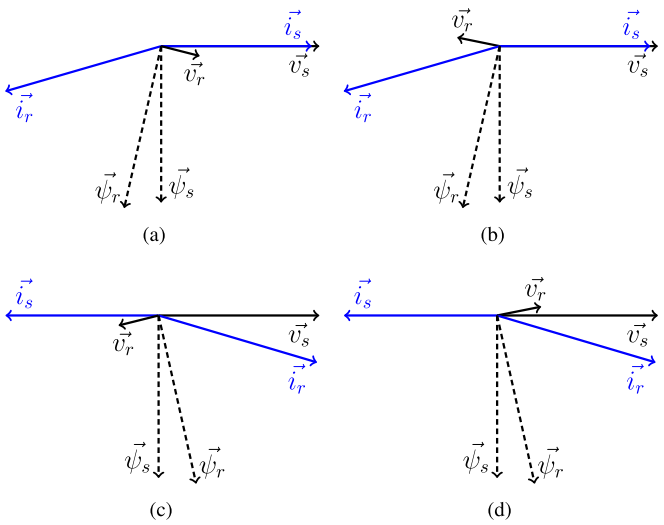

Fig. 2. Phasor diagram for four-quadrant operation of DFIM using existing equivalent circuit. (a) Motor ($\omega_r < \omega_s$). (b) Motor ($\omega_r > \omega_s$). (c) Generator ($\omega_r < \omega_s$). (d) Generator ($\omega_r > \omega_s$).

When the machine is operating at supersynchronous speed $\omega_r > \omega_s$, the results (shown in Table I) obtained using existing equivalent circuit show that the reactive power on the rotor side is negative ($Q_r < 0$), indicating that the DFIM is supplying reactive power back to the grid from the rotor side. This can further be verified from phasor diagrams indicated in Fig. 2(b) and (c) where the rotor current $\vec{i_r}$ is leading the rotor voltage $\vec{v_r}$.

This is counterintuitive, as the result does not clearly indicate the source of magnetizing power (reactive in nature). When the machine is operating in UPF mode, it is expected that the reactive power required to magnetize the core is drawn from the rotor side. The results obtained using the existing equivalent indicate otherwise.

III. ACCURATE EQUIVALENT CIRCUIT OF DFIM

Starting from the dynamic equations of DFIM, a step-by-step procedure to obtain an accurate steady-state phasor representation of DFIM is presented in this section. The conventions employed in deriving the model for DFIM are as follows.

1) The model is derived based on a synchronously rotating frame of reference $dq0$ and the q-axis is assumed to be leading the d-axis by $\frac{\pi}{2}$ in the direction of rotation.
2) The machine equations are derived assuming a motor convention.

Using the above conventions, a mathematical model for DFIM (under balanced operating conditions) in $dq0$ reference frame is given by the set of differential equations

$$\begin{aligned}
\frac{\partial \psi_{ds}}{\partial t} - \omega_s \psi_{qs} + R_s i_{ds} &= v_{ds} \\
\frac{\partial \psi_{qs}}{\partial t} + \omega_s \psi_{ds} + R_s i_{qs} &= v_{qs} \\
\frac{\partial \psi_{dr}}{\partial t} - (\omega_s - \omega_r)\psi_{qr} + R_r i_{dr} &= v_{dr} \\
\frac{\partial \psi_{qr}}{\partial t} + (\omega_s - \omega_r)\psi_{dr} + R_r i_{qr} &= v_{qr} \\
J\frac{\partial^2 \beta_r}{\partial t^2} &= \left([\psi_{ds} i_{qs} - \psi_{qs} i_{ds}] - T_m\right). \qquad (1)
\end{aligned}$$

The relationship between flux and current in various winding's in synchronously rotating frame of reference is given as

$$\begin{aligned}
\psi_{ds} &= L_s i_{ds} + L_m i_{dr} \\
\psi_{qs} &= L_s i_{qs} + L_m i_{qr} \\
\psi_{dr} &= L_r i_{dr} + L_m i_{ds} \\
\psi_{qr} &= L_r i_{qr} + L_m i_{qs} \qquad (2)
\end{aligned}$$

where $L_s = L_m + L_{\sigma s}$ and $L_r = L_m + L_{\sigma r}$.

Under steady-state operation ($\dot{\psi}_{ds} = \dot{\psi}_{qs} = \dot{\psi}_{dr} = \dot{\psi}_{qr} = 0$), the differential equations transform themselves as algebraic equations. Further, if the machine is assumed to be balanced (no zero-sequence components), the equations describing the behavior of DFIM under steady-state can be written as

$$\begin{aligned}
v_{ds} &= [-\omega_s \psi_{qs} + R_s i_{ds}] \\
v_{qs} &= [\omega_s \psi_{ds} + R_s i_{qs}] \\
v_{dr} &= [-s\omega_s \psi_{qr} + R_r i_{dr}] \\
v_{qr} &= [s\omega_s \psi_{dr} + R_r i_{qr}]. \qquad (3)
\end{aligned}$$

To obtain a steady-state equivalent circuit, the equations of DFIM under steady state in synchronously rotating frame of reference [$dq0$ reference frame, given by (3)] must be transformed into the stationary frame of reference of stator. This can be achieved using the Park's transformation matrix. During this transformation, attention must be paid in particular to the phase sequence in the rotor side. In view of this, we propose an accurate steady-state model for two scenarios namely (a) subsynchronous mode, and (b) supersynchronous mode.

A. Equivalent Circuit for Subsynchronous Mode of Operation

The $dq0$ components of stator quantities can be obtained using Park's transformation matrix $\mathbf{T_s}(\beta_s)$. For instance, the $dq0$ components of stator voltage ($\vec{v_s} = V_s \angle \theta_s$) under balanced

steady-state operation can be computed using

$$\begin{bmatrix} v_{ds} & v_{qs} & v_{0s} \end{bmatrix}^t = \sqrt{\frac{2}{3}} \begin{bmatrix} \cos(\beta_s) & \cos(\beta_s - \frac{2\pi}{3}) & \cos(\beta_s + \frac{2\pi}{3}) \\ -\sin(\beta_s) & -\sin(\beta_s - \frac{2\pi}{3}) & -\sin(\beta_s + \frac{2\pi}{3}) \\ \sqrt{\frac{1}{2}} & \sqrt{\frac{1}{2}} & \sqrt{\frac{1}{2}} \end{bmatrix} \times \begin{bmatrix} V_{sm}\cos(\omega_s t + \theta_s) \\ V_{sm}\cos(\omega_s t + \theta_s - \frac{2\pi}{3}) \\ V_{sm}\cos(\omega_s t + \theta_s + \frac{2\pi}{3}) \end{bmatrix}. \quad (4)$$

In (4), V_{sm} represents the peak value of phase to neutral voltage applied at stator terminals. Simplification of (4) gives

$$\begin{aligned} v_{ds} &= V_s \cos(\omega_s t + \theta_s - \beta_s) \\ v_{qs} &= V_s \sin(\omega_s t + \theta_s - \beta_s) \end{aligned} \quad (5)$$

where V_s is the line-to-line rms voltage. Under steady state, $\beta_s = \omega_s t$ and consequently, to obtain a relationship between components of stator voltage in synchronous and stationary frames of reference, consider

$$v_{ds} + jv_{qs} = V_s \left[e^{j(\omega_s t + \theta_s - \beta_s)} \right] = \vec{v_s}. \quad (6)$$

Analogously, the relationship between components of stator flux (and current) in synchronous and stationary frames of reference can be written as

$$\begin{aligned} i_{ds} + ji_{qs} &= \vec{i_s} \\ \psi_{ds} + j\psi_{qs} &= \vec{\psi_s}. \end{aligned} \quad (7)$$

The $dq0$ components of rotor quantities can be obtained using Park's transformation matrix $\mathbf{T_r}(\beta_\mathbf{s} - \beta_\mathbf{r})$. For instance, the $dq0$ components of rotor voltage ($\vec{v_r} = V_r \angle \theta_r$) under balanced steady-state operation can be computed using (8), shown at the bottom of the page. In (8), V_{rm} represents the peak value of phase to neutral voltage applied at rotor terminals. Simplification of (8) results in

$$\begin{aligned} v_{dr} &= V_r \cos((\omega_s - \omega_r)t + \theta_r - (\beta_s - \beta_r)) \\ v_{qr} &= V_r \sin((\omega_s - \omega_r)t + \theta_r - (\beta_s - \beta_r)). \end{aligned} \quad (9)$$

where V_r is the line-to-line rms voltage. To obtain a relationship between components of rotor voltage in synchronous and stationary frames of reference, consider

$$\begin{aligned} v_{dr} + jv_{qr} &= V_r \left[e^{j((\omega_s - \omega_r)t + \theta_r - (\beta_s - \beta_r))} \right] \\ &= V_r e^{j\theta_r} e^{j(\omega_s t + \beta_s)} e^{j(-\omega_r t + \beta_r)}. \end{aligned} \quad (10)$$

Under steady-state operation, $\beta_r = \omega_r t$ and as a result, (10) can further be simplified as

$$v_{dr} + jv_{qr} = \vec{v_r} \quad (11)$$

where $\vec{v_r}$ is the phasor representation of rotor voltage referred to stator side. Using (11), the relationship between rotor flux (and current) in synchronous and stationary frames of reference can be written analogously as

$$\begin{aligned} i_{dr} + ji_{qr} &= \vec{i_r} \\ \psi_{dr} + j\psi_{qr} &= \vec{\psi_r}. \end{aligned} \quad (12)$$

From (2), (7), and (12) , the stator and rotor flux can be expressed in terms of currents in stationary frame of reference as

$$\begin{aligned} \vec{\psi_s} &= [\psi_{ds} + j\psi_{qs}] \\ &= [L_s(i_{ds} + ji_{qs}) + L_m(i_{dr} + ji_{qr})] \\ \vec{\psi_s} &= L_s\vec{i_s} + L_m\vec{i_r} = L_{\sigma s}\vec{i_s} + L_m\left(\vec{i_s} + \vec{i_r}\right) \\ \vec{\psi_r} &= [\psi_{dr} + j\psi_{qr}] \\ &= [L_r(i_{dr} + ji_{qr}) + L_m(i_{ds} + ji_{qs})] \\ \vec{\psi_r} &= L_r\vec{i_r} + L_m\vec{i_s} = L_{\sigma r}\vec{i_r} + L_m\left(\vec{i_r} + \vec{i_s}\right). \end{aligned} \quad (13)$$

Using (3), (6), and (7), the steady-state behavior of stator in stationary frame of reference can be written mathematically as

$$\begin{aligned} \vec{v_s} &= (v_{ds} + jv_{qs}) \\ \vec{v_s} &= [(-\omega_s\psi_{qs} + R_s i_{ds}) + j(\omega_s\psi_{ds} + R_s i_{qs})] \\ \vec{v_s} &= [R_s(i_{ds} + ji_{qs}) + j\omega_s(\psi_{ds} + j\psi_{qs})] \\ \vec{v_s} &= R_s\vec{i_s} + j\omega_s\vec{\psi_s}. \end{aligned} \quad (14)$$

Similarly, the mathematical relationship describing the steady-state behavior of rotor in stationary frame of reference can be obtained using (3), (11), and (12)

$$\begin{aligned} \vec{v_r} &= (v_{dr} + jv_{qr}) \\ \vec{v_r} &= [(-s\omega_s\psi_{qr} + R_r i_{dr}) + j(s\omega_s\psi_{dr} + R_r i_{qr})] \\ \vec{v_r} &= [R_r(i_{dr} + ji_{qr}) + js\omega_s(\psi_{dr} + j\psi_{qr})] \\ \vec{v_r} &= R_r\vec{i_r} + js\omega_s\vec{\psi_r}. \end{aligned} \quad (15)$$

Finally, using (13)–(15), a mathematical model for DFIM in terms of voltages and currents can be written as

$$\begin{aligned} \vec{v_s} &= R_s\vec{i_s} + jX_{\sigma s}\vec{i_s} + jX_m\left(\vec{i_s} + \vec{i_r}\right) \\ \vec{v_r} &= R_r\vec{i_r} + jsX_{\sigma r}\vec{i_r} + jsX_m\left(\vec{i_r} + \vec{i_s}\right). \end{aligned} \quad (16)$$

$$\begin{bmatrix} v_{dr} \\ v_{qr} \\ v_{0r} \end{bmatrix} = \sqrt{\frac{2}{3}} \begin{bmatrix} \cos(\beta_s - \beta_r) & \cos(\beta_s - \beta_r - \frac{2\pi}{3}) & \cos(\beta_s - \beta_r + \frac{2\pi}{3}) \\ -\sin(\beta_s - \beta_r) & -\sin(\beta_s - \beta_r - \frac{2\pi}{3}) & -\sin(\beta_s - \beta_r + \frac{2\pi}{3}) \\ \sqrt{\frac{1}{2}} & \sqrt{\frac{1}{2}} & \sqrt{\frac{1}{2}} \end{bmatrix} \begin{bmatrix} V_{rm}\cos((\omega_s - \omega_r)t + \theta_r) \\ V_{rm}\cos((\omega_s - \omega_r)t + \theta_r - \frac{2\pi}{3}) \\ V_{rm}\cos((\omega_s - \omega_r)t + \theta_r + \frac{2\pi}{3}) \end{bmatrix} \quad (8)$$

The set of equations given by (16) can be represented by an equivalent circuit shown in Fig. 1 which is the same as the one proposed in the literature.

B. Equivalent Circuit for Supersynchronous Mode of Operation

When the DFIM is operating at supersynchronous speeds, the phase sequence on the rotor side is reversed, while the phase sequence on the stator side is in the usual order. Hence, the relationship between stator quantities in synchronous and stationary frames of reference is the same as that obtained for subsynchronous mode of operation [given by (6) and (7)]. However, for the quantities on the rotor side, the effect of phase reversal needs to be considered. It is to be noted that, under supersynchronous mode of operation, the frequency of voltage applied at the rotor terminals is $\omega_r - \omega_s$. In addition, the reference frame of rotor (spatial position given by β_r) leads the synchronously rotating frame of reference. Taking these aspects into consideration, the components of rotor voltage in rotating frame of reference can be computed using (17) as shown at the bottom of the page. Simplification of (17) results in

$$\begin{aligned} v_{dr} &= V_r \cos\left(\left(\omega_s - \omega_r\right) t + \theta_r - \left(\beta_s - \beta_r\right)\right) \\ v_{qr} &= -V_r \sin\left(\left(\omega_s - \omega_r\right) t + \theta_r - \left(\beta_s - \beta_r\right)\right). \end{aligned} \quad (18)$$

Comparison of (18) with (9) indicates that under supersynchronous mode of operation, the value of q-axis component is negative of that obtained during subsynchronous mode of operation. Accordingly, the relationship between components of rotor quantities in $dq0$ reference frame and stationary frame of reference is given as

$$\begin{aligned} v_{dr} - jv_{qr} &= V_r \left[e^{j\left(\left(\omega_s - \omega_r\right) t + \theta_r - \left(\beta_s - \beta_r\right)\right)}\right] \\ v_{dr} - jv_{qr} &= \vec{v_r}. \end{aligned} \quad (19)$$

By analogy, the relationship between components of rotor flux (and current) in synchronous and stationary frames of reference at supersynchronous speeds can be written as

$$\begin{aligned} i_{dr} - ji_{qr} &= \vec{i_r} \\ \psi_{dr} - j\psi_{qr} &= \vec{\psi_r}. \end{aligned} \quad (20)$$

During supersynchronous mode of operation, the stator flux in stationary frame of reference can be expressed in terms of currents as [using (2), (7), and (20)]

$$\begin{aligned} \vec{\psi_s} &= \left[\psi_{ds} + j\psi_{qs}\right] \\ &= \left[L_s\left(i_{ds} + ji_{qs}\right) + L_m\left(i_{dr} + ji_{qr}\right)\right] \\ \vec{\psi_s} &= L_s\vec{i_s} + L_m\vec{i_r}^{*} = L_{\sigma s}\vec{i_s} + L_m\left(\vec{i_s} + \vec{i_r}^{*}\right). \end{aligned} \quad (21)$$

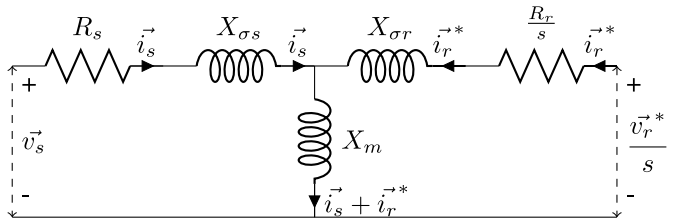

Fig. 3. Accurate steady-state representation of DFIM operating at supersynchronous speeds.

Similarly, the rotor flux in stationary frame of reference can be expressed in terms of currents as

$$\begin{aligned} \vec{\psi_r} &= \left[\psi_{dr} - j\psi_{qr}\right] \\ &= \left[L_r\left(i_{dr} - ji_{qr}\right) + L_m\left(i_{ds} - ji_{qs}\right)\right] \\ \vec{\psi_r} &= L_r\vec{i_r} + L_m\vec{i_s}^{*} = L_{\sigma r}\vec{i_r} + L_m\left(\vec{i_r} + \vec{i_s}^{*}\right). \end{aligned} \quad (22)$$

Since the phase sequence on the stator side in unaltered at supersynchronous speeds, the mathematical relationship describing the relationship between flux and voltage of stator at supersynchronous speeds is given by (14). However, for the rotor circuit, the mathematical relationship is different to that obtained for subsynchronous mode of operation. For supersynchronous mode of operation, the mathematical relationship describing the steady-state behavior of rotor is given as [using (3), (19), and (22)]

$$\begin{aligned} \vec{v_r} &= \left(v_{dr} - jv_{qr}\right) \\ \vec{v_r} &= \left[\left(-s\omega_s\psi_{qr} + R_r i_{dr}\right) - j\left(s\omega_s\psi_{dr} + R_r i_{qr}\right)\right] \\ \vec{v_r} &= \left[R_r\left(i_{dr} - ji_{qr}\right) - js\omega_s\left(\psi_{dr} - j\psi_{qr}\right)\right] \\ \vec{v_r} &= R_r\vec{i_r} - js\omega_s\vec{\psi_r}. \end{aligned} \quad (23)$$

Though the relationship between stator voltage and stator flux is the same for both subsynchronous and supersynchronous modes of operation, the relationship between stator flux and currents is different (21). As a result, the mathematical relationship describing the steady-state behavior of stator is different for the two modes of operation. Using (21)–(23), a mathematical model for DFIM operating in supersynchronous mode can be written as

$$\vec{v_s} = R_s\vec{i_s} + jX_{\sigma s}\vec{i_s} + jX_m\left(\vec{i_s} + \vec{i_r}^{*}\right) \quad (24a)$$

$$\vec{v_r} = R_r\vec{i_r} - jsX_{\sigma r}\vec{i_r} - jsX_m\left(\vec{i_r} + \vec{i_s}^{*}\right). \quad (24b)$$

$$\begin{bmatrix} v_{dr} \\ v_{qr} \\ v_{0r} \end{bmatrix} = \sqrt{\frac{2}{3}} \begin{bmatrix} \cos(\beta_r - \beta_s) & \cos(\beta_r - \beta_s - \frac{2\pi}{3}) & \cos(\beta_r - \beta_s + \frac{2\pi}{3}) \\ -\sin(\beta_r - \beta_s) & -\sin(\beta_r - \beta_s - \frac{2\pi}{3}) & -\sin(\beta_r - \beta_s + \frac{2\pi}{3}) \\ \sqrt{\frac{1}{2}} & \sqrt{\frac{1}{2}} & \sqrt{\frac{1}{2}} \end{bmatrix} \begin{bmatrix} V_{rm}\cos\left(\left(\omega_r - \omega_s\right)t + \theta_r\right) \\ V_{rm}\cos\left(\left(\omega_r - \omega_s\right)t + \theta_r + \frac{2\pi}{3}\right) \\ V_{rm}\cos\left(\left(\omega_r - \omega_s\right)t + \theta_r - \frac{2\pi}{3}\right) \end{bmatrix} \quad (17)$$

TABLE II
SUMMARY OF STATOR AND ROTOR EQUATIONS OF DFIM (BASED ON PROPOSED MODEL)

Mode	Stator	Rotor
$\omega_r < \omega_s$	$\vec{v_s} = R_s\vec{i_s} + jX_{\sigma s}\vec{1_s} + jX_m\left(\vec{i_s} + \vec{i_r}\right)$	$\frac{\vec{v_r}}{s} = \frac{R_r}{s}\vec{i_r} + jX_{\sigma r}\vec{i_r} + jX_m\left(\vec{i_r} + \vec{i_s}\right)$
	$S_s = \sqrt{3}\vec{v_s}\vec{i_s}^* = \sqrt{3}\left(v_{ds} + jv_{qs}\right)\left(i_{ds} + ji_{qs}\right)^*$	$S_r = \sqrt{3}\vec{v_r}\vec{i_r}^* = \sqrt{3}\left(v_{dr} + jv_{qr}\right)\left(i_{dr} + ji_{qr}\right)^*$
	$P_s = \text{Re}(\sqrt{3}\vec{v_s}\vec{i_s}^*) = \sqrt{3}\left(v_{ds}i_{ds} + v_{qs}i_{qs}\right)$	$P_r = \text{Re}(\sqrt{3}\vec{v_r}\vec{i_r}^*) = \sqrt{3}\left(v_{dr}i_{dr} + v_{qr}i_{qr}\right)$
	$Q_s = \text{Im}(\sqrt{3}\vec{v_s}\vec{i_s}^*) = \sqrt{3}\left(v_{qs}i_{ds} - v_{ds}i_{qs}\right)$	$Q_r = \text{Im}(\sqrt{3}\vec{v_r}\vec{i_r}^*) = \sqrt{3}\left(v_{qr}i_{dr} - v_{dr}i_{qr}\right)$
$\omega_r > \omega_s$	$\vec{v_s} = R_s\vec{i_s} + jX_{\sigma s}\vec{1_s} + jX_m\left(\vec{i_s} + \vec{i_r}^*\right)$	$\frac{\vec{v_r}^*}{s} = \frac{R_r}{s}\vec{i_r}^* + jX_{\sigma r}\vec{i_r}^* + jX_m\left(\vec{i_r}^* + \vec{i_s}\right)$
	$S_s = \sqrt{3}\vec{v_s}\vec{i_s}^* = \sqrt{3}\left(v_{ds} + jv_{qs}\right)\left(i_{ds} + ji_{qs}\right)^*$	$S_r = \sqrt{3}\vec{v_r}\vec{i_r}^* = \sqrt{3}\left(v_{dr} - jv_{qr}\right)\left(i_{dr} - ji_{qr}\right)^*$
	$P_s = \text{Re}(\sqrt{3}\vec{v_s}\vec{i_s}^*) = \sqrt{3}\left(v_{ds}i_{ds} + v_{qs}i_{qs}\right)$	$P_r = \text{Re}(\sqrt{3}\vec{v_r}\vec{i_r}^*) = \sqrt{3}\left(v_{dr}i_{dr} + v_{qr}i_{qr}\right)$
	$Q_s = \text{Im}(\sqrt{3}\vec{v_s}\vec{i_s}^*) = \sqrt{3}\left(v_{qs}i_{ds} - v_{ds}i_{qs}\right)$	$Q_r = \text{Im}(\sqrt{3}\vec{v_r}\vec{i_r}^*) = -\sqrt{3}\left(v_{qr}i_{dr} - v_{dr}i_{qr}\right)$

TABLE III
ANALYSIS OF FOUR-QUADRANT OPERATION OF DFIM USING PROPOSED EQUIVALENT CIRCUIT[1] ($Q_s = 0$, $s = \pm 0.25$) (ALL VALUES ARE IN P.U.)

Quad	ω_r	P_s	P_r	Q_r	P_m	T_m
A	$\omega_r < \omega_s$	0.95	−0.22	0.13	0.73	0.94
B	$\omega_r > \omega_s$	0.95	0.25	**0.13**	1.20	0.94
C	$\omega_r > \omega_s$	−0.95	−0.22	**0.13**	−1.18	−0.96
D	$\omega_r < \omega_s$	−0.95	0.25	0.13	−0.70	−0.96

The equations can be rewritten in an alternate manner [by taking complex conjugate on both sides of (24b)] as

$$\begin{aligned}\vec{v_s} &= R_s\vec{i_s} + jX_{\sigma s}\vec{1_s} + jX_m\left(\vec{i_s} + \vec{i_r}^*\right)\\ \frac{\vec{v_r}^*}{s} &= \frac{R_r}{s}\vec{i_r}^* + jX_{\sigma r}\vec{i_r}^* + jX_m\left(\vec{i_r}^* + \vec{i_s}\right).\end{aligned} \quad (25)$$

Using the above set of equations, the equivalent steady-state model for DFIM operating at supersynchronous speeds can be represented as shown in Fig. 3.

The equations describing the behavior of stator and rotor of DFIM at both subsynchronous and supersynchronous speeds are summarized in Table II. In addition, the mathematical relations to compute the active and reactive power at stator and rotor terminals are also indicated. It can be noted that the mathematical expressions to compute the reactive power flow in the rotor side is different for subsynchronous and supersynchronous modes of operation. In fact, the expressions to compute Q_r are negative of each other. If the existing equivalent circuit is used to analyze the behavior of DFIM, the equations describing the behavior of rotor and the expression for Q_r would be the same for both subsynchronous and supersynchronous modes of operation which is not true.

IV. ANALYSIS OF THE PROPOSED EQUIVALENT CIRCUIT

To illustrate the validity of the proposed equivalent circuits (Fig. 1 for subsynchronous speeds and Fig. 3 for supersynchronous speeds), a 2-MW DFIM is analyzed for its four-quadrant operation. The results obtained are tabulated in Table III and the corresponding phasor diagrams are indicated in Fig. 4. It can be seen that the reactive power required to magnetize the core (especially when the DFIM is operating in UPF mode at supersynchronous speeds) is drawn from the rotor side. This can further be verified from the phasor diagrams presented in Fig. 4, where $\vec{v_r}$ is leading $\vec{i_r}$ during its operation in all the four quadrants. Further, the phasor diagrams (shown in Fig. 4) indicate that for the same power and voltage at stator terminals, the current and the flux in the rotor side during supersynchronous mode of operation are the complex conjugate of their respective values obtained during subsynchronous mode of operation.

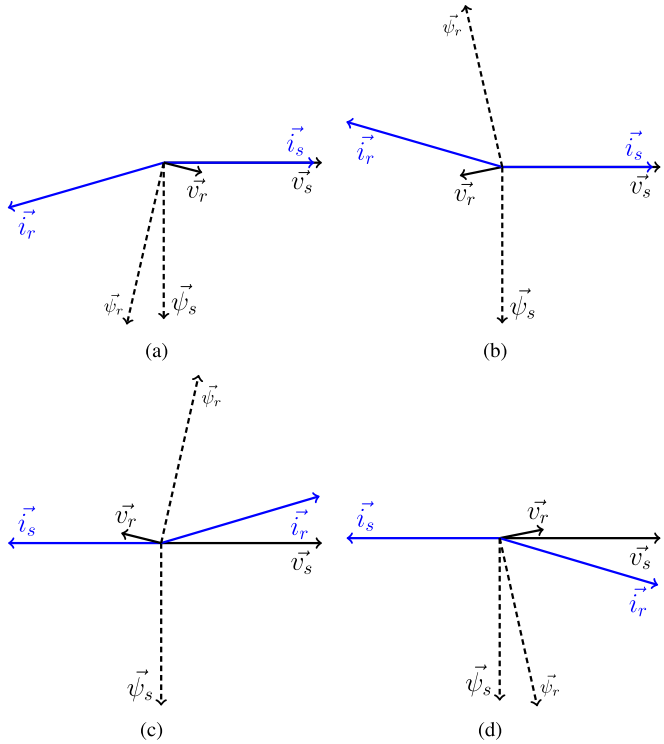

Fig. 4. Phasor diagram for four-quadrant operation of DFIM using proposed equivalent circuit. (a) Motor ($\omega_r < \omega_s$). (b) Motor ($\omega_r > \omega_s$). (c) Generator ($\omega_r < \omega_s$). (d) Generator ($\omega_r > \omega_s$).

To validate the proposed equivalent circuit further, the reactive power requirement at the rotor terminals for different values of Q_s during supersynchronous mode of operation (both as a generator and motor) is indicated in Fig. 5. For this scenario, the active power at the stator side is presumed to

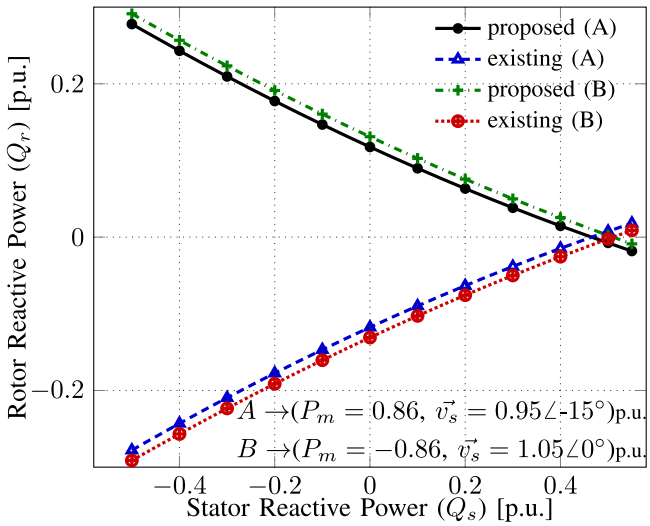

Fig. 5. Q_s versus Q_r for DFIM operating at supersynchronous speeds ($s = -0.25$) for two operating points A ($P_m = 0.86$p.u. and $\vec{v_s} = 0.95\angle -15°$p.u.) and B($P_m = -0.86$p.u. and $\vec{v_s} = 1.05\angle 0°$p.u.).

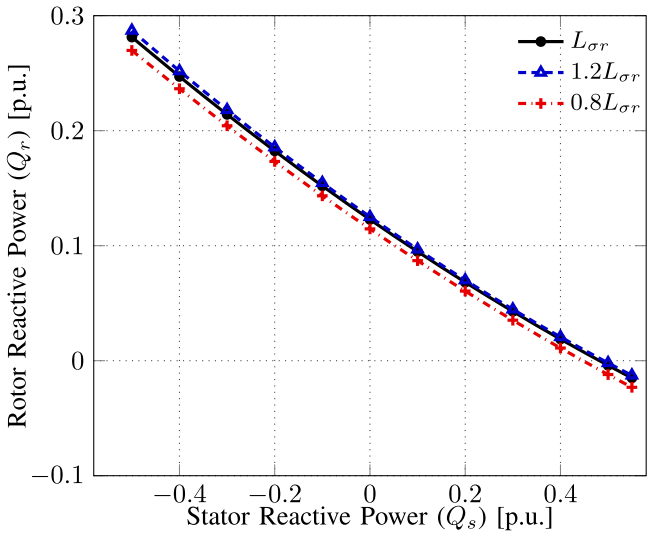

Fig. 6. Impact of variation of $L_{\sigma r}$ for DFIM operating at supersynchronous speeds as a generator with $P_s = -1.8$ **MW** and $\vec{v_s} = 1.00\angle 0$.

be ± 1.8 MW(≈ 0.86 p.u.). The stator voltage is presumed to be $0.95\angle -15°$ p.u. and $1.05\angle 0$ p.u. during its motoring and generating modes, respectively. When the DFIM is supplying reactive power to the grid ($Q_s < 0$), the necessary reactive power must be absorbed from the rotor side ($Q_r > 0$). It can be verified from Fig. 5, that the reactive power flow direction ($Q_r > 0$ when $Q_s < 0$) is accurately predicted using the proposed equivalent.

To indicate the effect of machine parameters [13] (varying due to temperature and saturation effects) on the steady-state behavior (computed reactive power flow directions using proposed equivalent), the impact of variation in $L_{\sigma r}$ on computed Q_r is illustrated in Fig. 6. It can be observed that the impact of variation of machine parameters on computed reactive power flow directions is minimal.

V. Conclusion

In this letter, it is shown that the equivalent circuit of DFIM proposed in the literature is inaccurate for analyzing the steady-state behavior at supersynchronous speeds. The primary reason can be attributed to phase sequence reversal in rotor side, which is not properly accounted in the existing equivalent circuit. An accurate steady-state representation of DFIM operating at supersynchronous speeds considering phase sequence reversal is proposed and is further validated on a 2-MW DFIM. Analysis using the proposed model indicates that, for the same power and voltage at stator terminals, the flux and current in the rotor side during supersynchronous mode of operation are the complex conjugate of their respective values obtained during subsynchronous mode of operation.

Appendix

A. Parameters of 2-MW DFIM

$R_s = 2.6$ mΩ; $R_r = 2.9$ mΩ; 50 Hz, $p = 2$, $L_{\sigma s} = 0.087$ mH; $L_{\sigma r} = 0.087$ mH; L_m=2.5 mH $S_{\text{base}} = 2.1$ MVA; $V_{\text{base}} = 690$ V (line-to-line, rms).

References

[1] S. Muller, M. Deicke, and R. W. De Doncker, "Doubly fed induction generator systems for wind turbines," *IEEE Ind. Appl. Mag.*, vol. 8, no. 3, pp. 26–33, May/Jun. 2002.

[2] J. M. Carrasco, L. G. Franquelo, J. T. Bialasiewicz, E. Galván, R. P. Guisado, M. A. Prats, J. I. León, and N. Moreno-Alfonso, "Power-electronic systems for the grid integration of renewable energy sources: A survey," *IEEE Trans. Ind. Electron.*, vol. 53, no. 4, pp. 1002–1016, Jun. 2006.

[3] R. Pena, J. Clare, and G. Asher, "Doubly fed induction generator using back-to-back pwm converters and its application to variable-speed wind-energy generation," *Proc. IEE -Electr. Power Appl.*, vol. 143, no. 3, pp. 231–241, May 1996.

[4] G. Abad, J. Lopez, M. Rodríguez, L. Marroyo, and G. Iwanski, *Doubly Fed Induction Machine: Modeling and Control for Wind Energy Generation*. New York, NY, USA: Wiley, 2011, vol. 86.

[5] B. Wu, Y. Lang, N. Zargari, and S. Kouro, *Power Conversion and Control of Wind Energy Systems*. New York: Wiley, 2011, vol. 77.

[6] V. Vittal and R. Ayyanar, *Grid Integration and Dynamic Impact of Wind Energy*. New York, NY, USA: Springer-Verlag, 2013.

[7] F. K. Lima, A. Luna, P. Rodriguez, E. H. Watanabe, and F. Blaabjerg, "Rotor voltage dynamics in the doubly fed induction generator during grid faults," *IEEE Trans. Power Electron.*, vol. 25, no. 1, pp. 118–130, Jan. 2010.

[8] A. Luna, F. d. A. Lima, D. Santos, P. Rodríguez, E. H. Watanabe, and S. Arnaltes, "Simplified modeling of a DFIG for transient studies in wind power applications," *IEEE Trans. Ind. Electron.*, vol. 58, no. 1, pp. 9–20, Jan. 2011.

[9] M. El Moursi, G. Joos, and C. Abbey, "A secondary voltage control strategy for transmission level interconnection of wind generation," *IEEE Trans. Power Electron.*, vol. 23, no. 3, pp. 1178–1190, May 2008.

[10] S. Hu, X. Lin, Y. Kang, and X. Zou, "An improved low-voltage ride-through control strategy of doubly fed induction generator during grid faults," *IEEE Trans. Power Electron.*, vol. 26, no. 12, pp. 3653–3665, Dec. 2011.

[11] H. Nian and Y. Song, "Direct power control of doubly fed induction generator under distorted grid voltage," *IEEE Trans. Power Electron.*, vol. 29, no. 2, pp. 894–905, Feb. 2014.

[12] Y. Zhang, J. Hu, and J. Zhu, "Three-vectors-based predictive direct power control of the doubly fed induction generator for wind energy applications," *IEEE Trans. Power Electron.*, vol. 29, no. 7, pp. 3485–3500, Jul. 2014.

[13] R. Krishnan and F. C. Doran, "Study of parameter sensitivity in high-performance inverter-fed induction motor drive systems," *IEEE Trans. Ind. Appl.*, vol. 23, no. 4, pp. 623–635, Jul. 1987.